

Advances in air quality monitoring via nanotechnology

Marie-Isabelle Baraton¹ and Lhadi Merhari²

¹SPCTS - UMR6638 CNRS, Faculty of Sciences, University of Limoges, 123 Avenue Albert Thomas, F-87060 Limoges, France (Tel.: +33 555 45 7348; Fax: +33 555 77 8100; E-mail: baraton@unilim.fr);

²CERAMEC R&D, 64 Avenue de la Libération, F-87000 Limoges, France

Received 10 October 2003; accepted in revised form 17 December 2003

Key words: chemical gas sensors, environment monitoring, air quality monitoring, semiconducting nanoparticles, surface chemistry, polluting gases

Abstract

Urban air pollution has become an inescapable issue due to its serious consequences on public health and, therefore, needs more accurate tracking through denser networks of air quality monitoring (AQM) stations. A higher density of these networks can be afforded by cities only if the costs of future individual AQM stations decrease. We review here the outcome of two European projects where our objective was to provide an alternative approach consisting in the development of cost-effective mobile microstations based on semiconductor sensors and capable of complementing the expensive and bulky current AQM stations. Improvement of the sensor sensitivity to detect very low levels of pollutants (CO, NO, NO₂, O₃) in air was the major challenge to take up. This was achieved by using metal oxide nanosized particles with both controlled size and surface chemistry, and by adapting the screen-printing process to the nanometer size specificity. The detection thresholds for NO₂, NO and O₃ of our nanoparticles-based sensors have been decreased by a factor of 3–5 compared to currently commercialized sensors. The lowest detectable concentration of CO has been reduced from 5 to 3 ppm without affecting the selectivity. In terms of sensitivity performance, our sensor prototypes can now meet the criteria for outdoor AQM whereas the commercial semiconductor and electrochemical sensors still cannot. As for the implementation of the network as a whole, our technological approach is outlined.

Introduction: The INTAIRNET concept

Air pollution has been one of Europe's main political concerns since the late 1970s. But nowadays, the general public awareness of the consequences of urban air pollution on health has led decision-makers to define more drastic regulations for air quality monitoring (AQM). In 1996, the European Council adopted a Framework Directive on ambient air quality assessment and management (Directive 96/62/EC of 27/09/96) based on common methods and criteria in the EU Member States.¹ Then,

a series of Directives has been introduced to control levels of identified pollutants and to monitor their concentrations in air (e.g. among others: Directive 2000/69/EC of the European Parliament and of the Council of 16/11/2000; Directive 2001/81/CE of the European Parliament and of the Council of 23/10/2001; <http://europa.eu.int/eur-lex>). In the list of atmospheric pollutants to be considered, carbon monoxide (primary pollutant), nitrogen oxide and ozone (secondary pollutants) are explicitly mentioned.

The current European Union policy on air quality aims at developing and implementing appropriate instruments to monitor and improve air quality. European legislation also defines precise obligations, related to the information of the public in the event of significant pollution episodes such as

¹EU Member States as of 2003: Austria, Belgium, Denmark, Finland, France, Germany, Greece, Ireland, Italy, Luxembourg, Portugal, Spain, Sweden, The Netherlands, United Kingdom.

ozone exceedances. Besides, any European citizen has the right to demand national and local authorities to take action to improve the quality of air. As a consequence, every country of the European Union has been instructed to establish a network of AQM stations in its main cities and to inform citizens about the air quality on a daily basis.

In the current AQM stations, the ambient air is sampled, pumped in and carried toward the analyzers (one analyzer per gas). The data are transmitted to the central computer about four times per day on an average. Then, these data are processed and the concentration of each polluting gas is averaged over different periods of time (1 h, 8 h, 1 day, 1 week, etc). Finally, at the end of each day, the daily air quality index taking several factors into account is delivered to the public. The analyzers which are complex and bulky equipment, essentially based on electro-optical methods (UV and IR absorption), fluorescence or chemiluminescence, allow precise concentration measurements of different kinds of gaseous pollutants in air. However, it is clear that the lengthy air sampling and data processing do not allow 'real time' dissemination of the information to the public.

In addition, one of the major problems that cities are facing is the overall cost of the AQM stations which may reach up to several millions Euros for each unit. Only large and rich cities can afford them but, still, in an insufficient number for establishing a dense network and for obtaining a full coverage of the urban area: as an example, 45 automatic stations are spread over the Paris area (100 km-radius) representing 11 millions inhabitants, including the 12 stations located in the city of Paris.

Considering the growing concern about the impact of environment on quality of life and health, specially for children and seniors, the increasing public demand for transparency in the delivered information, the issues raised in terms of pollution monitoring by the acceding countries to the EU² including at cross-boundaries areas, we propose an alternative solution for affordable AQM. Our objective is to provide AQM systems based on cost-effective semiconductor gas sensors. By strongly reducing the cost of the stations, it will become possible to implement dense networks in every large city in every country. In addition, due

²Acceding countries to the EU: Cyprus, Czech Republic, Estonia, Hungary, Latvia, Lithuania, Malta, Poland, Slovakia and Slovenia.

to the tiny size of semiconductor sensors, it can be envisaged to integrate different sensors in small sensing units, thus transforming the bulky expensive AQM stations into cost-effective portable devices. But, to this end, the performance of the semiconductor gas sensors have to be enhanced, specially in terms of high sensitivity to gases and low cross-sensitivity to humidity.

In a second step, these portable gas sensing units will communicate with a central computer via a wireless network based on the GSM protocol. Additionally, these sensing units will be associated to global positioning systems (GPS). The resulting communicating microstations, installed on mobile carriers such as city buses, will constitute a dynamic network covering the city and complementing the existing AQM stations. Through the Internet, it therefore becomes possible to not only inform in quasi real time citizens on air quality status but also help decision-makers to more efficiently manage road traffic, provide scientists with additional data to refine mathematical models of pollution clouds in cities and inform hospitals in quasi real time about approaching pollution episodes. With the booming development of telecommunication networks and the recent integration of GSM and GPS technologies in commercially available devices, this second step of the project designed by our Consortium as early as the beginning of 1999 has now simply become the modification of existing systems for our specific application.

The sensing element represents the most challenging component in our concept of mobile AQM microstations and our proposed dynamic network is relevant only if cost-effective semiconductor sensors can successfully and reliably detect low gas concentrations and meet the detection threshold criteria set by the official organizations in charge of environment protection. To date, currently commercialized semiconductor sensors do not meet these criteria.

In two projects funded by the European Commission under the BRITE-EURAM III and IST programmes (Contracts SMOGLESS No BRPR-CT95-0002 and INTAIRNET IST-1999-12615), our Consortia worked on the improvement of the semiconductor gas sensor characteristics by using nanosized semiconductor particles for CO, NO, NO₂ and ozone detection. This article summarizes the different stages in our progress toward the improvement of the nanoparticle-based sensors, and the achievements of our Consortia to date.

Setting the problem

The official organizations in charge of the protection of our environment, such as the European Environment Agency in the European Union (<http://www.eea.eu.int>) and the Environment Protection Agency in the USA (<http://www.epa.gov>), have defined the maximum authorized concentrations of pollutants averaged over different periods of time. They are summarized in Table 1 for the most common polluting gases that we are considering in this work, namely CO, NO₂, NO and O₃. It clearly appears that any kind of instrument for measuring outdoor pollutant concentrations must be capable of reliably detecting these concentrations. In particular, gas sensors must have detection thresholds well below these authorized concentrations so that most of the pollution episodes can be accurately measured. To this end, in agreement with experts in environment protection, we have defined detection thresholds for CO, NO₂, NO and O₃ as targets that our sensor prototypes should meet at the end of our projects in order to comply with the EU directives (Table 1).

Currently, the most popular semiconductor gas sensors are commercialized by the Japanese company Figaro Engineering Incorporated (<http://www.figarosensor.com/>). Figaro gas sensors are solid-state devices composed of sintered metal oxides (mainly tin oxide, SnO₂). As all resistive gas sensors, they detect gases through variations of the electrical conductivity when reducing or oxidizing gases are adsorbed on the semiconductor surface (Morrison, 1994). Generally, the semiconductor sensors are very popular for indoor air quality control, due to their

low cost. However, they are not suitable for outdoor AQM because of their cross-sensitivity to humidity and their too high detection thresholds (Morrison, 1994).

To illustrate the improvements which had to be made, Table 1 compares our targeted detection thresholds with the typical sensitivities of commercial semiconductor and electrochemical sensors as available in 2000. It should be noted that electrochemical sensors are known to be more sensitive but much more expensive than semiconductor sensors. It is clear that none of the commercial sensors had sufficiently low detection thresholds for CO, NO₂, NO and O₃ to meet the EU requirements for outdoor AQM.

New paradigms for the advancement of semiconductor sensors

Advantage of using nanoparticles

In resistive sensors, the grain or crystallite size is one of the most important factors affecting the sensing properties. The first evidence was obtained in 1982 by Ogawa et al. (1982) from the measurements of the Hall parameters on SnO₂ nanoparticles. Ogawa et al. (1982) demonstrated that, when the grain size becomes comparable to twice the Debye length, the space-charge region can develop in the whole crystallite, thus resulting in a higher sensitivity to gases. For example, the sensitivity of sensors based on tin oxide nanoparticles dramatically increases when the particle size is reduced down to 6 nm. Below this critical grain size, the sensor sensitivity rapidly decreases

Table 1. Comparison between the gas detection thresholds required to detect the maximum authorized concentrations of pollutants in air and the gas detection thresholds of commercial sensors

Polluting gases	Maximum authorized concentrations in air		Target for the detection threshold	Detection thresholds of commercial sensors (typical data available in 2000)	
	EEA (EU)	EPA-OAQPS (USA)		Semiconductor	Electrochemical
CO	43 ppm (50 mg/m ³) $\frac{1}{2}$ h average	35 ppm (40 mg/m ³) 1 h average	3 ppm	100 ppm	5 ppm
NO ₂	105 ppb (200 µg/m ³) $\frac{1}{2}$ h average	53 ppb (100 µg/m ³) annual mean	50 ppb		600 ppb
NO	800 ppb (1000 µg/m ³) $\frac{1}{2}$ h average		100 ppb		900 ppb
O ₃	60 ppb (120 µg/m ³) $\frac{1}{2}$ h average	120 ppb (235 µg/m ³) 1 h average	20 ppb		200 ppb

(Shimizu & Egashira, 1999). As the calculated Debye length of SnO₂ is $D = 3$ nm at 250°C (Ogawa et al., 1982), the highest sensitivity is actually reached when the particle diameter corresponds to $2D$.

Besides, the surface reactivity of particles is known to rapidly increase with the increase of the surface-to-bulk ratio because the strong curvature of the particle surface generates a larger density of defects which are the most reactive surface sites (Somorjai, 1994). This high reactivity has largely been taken advantage of in catalysis where ultrafine particles have been used for decades. When properly processed during the fabrication of chemical semiconductor sensors, these nanoparticles are sufficiently reactive to make the use of catalytic additives (such as Pt or Pd) unnecessary (Panchapakesan et al., 2001) and to decrease the working temperature of the sensors without any loss of sensitivity. We have indeed experimentally proved that the use of nanosized semiconductor particles in the fabrication of chemical gas sensors via thick film technology greatly enhances the sensor sensitivity (Williams & Coles, 1998; Baraton & Merhari, 2001a).

Control of the physical and chemical properties of the nanoparticles

Several materials, including indium and tungsten oxide, were tested (Baraton et al., 2002), but our efforts essentially focused on tin oxide. Tin oxide is indeed the most popular material for gas sensing due to its relatively low cost and its high sensitivity.

Although, from the above-mentioned conclusions of Ogawa et al. (1982), 6 nm would be the optimum SnO₂ particle size for maximizing the sensor sensitivity, we very rapidly observed that the production yield of such particles by laser evaporation was too low to be commercially acceptable. An empirical approach led to the conclusion that the optimum balance between excellent sensor sensitivity and reasonable nanoparticle production yield (i.e. reasonable production costs) was reached for tin oxide particles having a diameter around 15 nm. Simultaneously, it clearly appeared that the nanoparticles had to be systematically controlled to exactly define the synthesis parameters, thus ensuring the reproducibility of the sensor characteristics over different batches. The particle size and shape, the particle size distribution, the crystalline state, the stoichiometry and the chemical composition were studied by transmission electron microscopy (TEM), X-ray diffraction (XRD)

spectrometry, energy dispersive X-ray analysis and Fourier transform infrared (FTIR) spectroscopy. In addition, the control of the surface chemistry of the nanoparticles was shown to be a key issue in the improvement of the sensor reliability and performance (Chancel et al., 1998). The surface chemistry was investigated by FTIR spectroscopy which was proved to be a very relevant technique to obtain a thorough understanding of the surface phenomena at the origin of the gas detection mechanism (Baraton & Merhari, 2000). This fundamental approach was considered as a critical step to refine the sensor optimization by tailoring both the surface chemical composition and reactivity of the nanoparticles during and eventually after their synthesis (Baraton & Merhari, 1998). It was also demonstrated that the systematic characterization of the nanoparticle surface at a chemical level guarantees the reproducibility of the sensor performance (Chancel et al., 1998).

Optimization of the screen-printing process

While the particle size reduction is an essential factor for sensitivity increase, it rapidly appeared that controlling this factor alone was not sufficient as the grain size had also to be retained during the entire sensor fabrication process. The usual method to fabricate thick-film gas sensors consists in dispersing the semiconducting particles in a suitable solvent (usually α -terpineol) to obtain an ink with appropriate viscosity (Williams & Coles, 1999). This ink is then printed on a substrate (generally an alumina tile) bearing electrodes with a heating element on the back side. The printed substrate is then dried and fired at controlled temperatures to avoid both shrinkage and film cracking (Williams & Coles, 1998). This standard procedure used for micron-sized particles had to be modified for nanoparticles in order to obtain a crack-free sensitive layer and to avoid grain growth. In particular, the firing step is critical for thick films based on nanoparticles and the firing temperature has to be carefully adjusted as discussed below. It was additionally concluded from experiments that the suppression of agglomerates should lead to improved adhesion and film quality where cracks due to inhomogeneous heat transfer cannot appear. By removing agglomerates, it was also expected that the resulting narrower particle size distribution would lead to a further sensitivity increase. The screen-printing process was therefore carefully adapted taking into account the specific and complex behavior of nanoparticles (Williams & Coles, 1998).

Results

Characterization of the nanoparticles

The SnO₂ nanoparticles were obtained by evaporating pellets made of compressed micropowder with the pulsed radiation of a Nd:YAG-laser, followed by nucleation of nanoparticles in a controlled aggregation gas (Riehemann, 1998). The chamber had to be kept under pure oxygen to avoid any contamination. The advantage of this synthesis method is that there is no contamination by non-dissociated precursors and there is no surface contaminant. As previously explained, we determined that an average particle diameter of 15 nm would ensure a good sensitivity at a reasonable production cost. Indeed, the production yield of such 15 nm-diameter particles is 5–10 g/h. The fabrication of about 1000 devices necessitates only 5–10 g of nanopowder.

The nanoparticles were analyzed using an X-ray diffractometer to determine both composition and particle size. The XRD spectrum revealed that the material was primarily tin dioxide (rutile phase) with some tin monoxide phase (Figure 1). The calculation of the mean diameter from the Scherrer formula gave a value of about 15 nm for tin dioxide particles. The average particle size was also determined by BET measurements giving a value of 13.3 nm. The size distribution was logarithmic normal with a geometric standard deviation of 1.7 (SMOGLASS Final Report, 1999). The TEM analysis (Figure 2) (Baraton et al., 2002) showed that the tin oxide nanoparticles of spherical shape were arranged in chains and that necks existed between some adjacent nanoparticles. A non-negligible degree of nanoparticle agglomeration was observed and had to be taken into account in the screen-printing process.

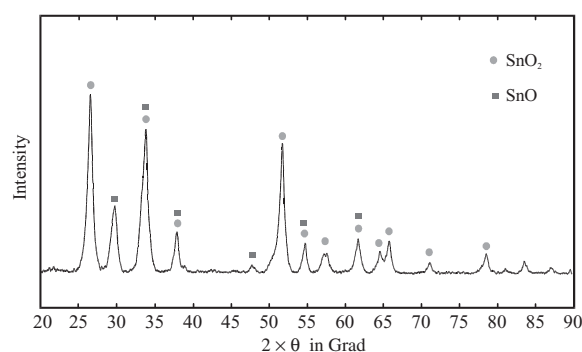


Figure 1. XRD analysis of the SnO₂ nanoparticles (particle diameter: 15 nm).

The infrared transmission spectrum of the tin oxide nanoparticles dispersed in potassium bromide and pressed into a pellet (Figure 3a) showed two main bands at 630 and 565 cm⁻¹ corresponding to the vibrations of the rutile structure in good agreement with literature data (Ocaña & Serna, 1991; Ocaña et al., 1993).

Surface chemistry of the nanoparticles

The reproducibility of the surface chemical composition and of the surface reactivity of nanoparticles has been proved to be crucial in all applications (Baraton, 1999). This is particularly critical in the case of gas sensors where the surface reactions are at the origin of the gas detection mechanism.

The surface chemistry of nanoparticles can be conveniently investigated by FTIR spectroscopy under specific conditions (Baraton, 1999). The infrared spectrum of the chemical groups at the very surface of the SnO₂ nanoparticles is presented in Figure 3b. All the absorption bands in the 4000–3000 cm⁻¹ region are due to the stretching vibrations of the OH groups bonded to tin atoms of the first atomic layer (Thornton & Harrison, 1975). The corresponding δ(OH) bending vibrations of these OH groups can be observed in the 1500–1000 cm⁻¹ region (Tribout et al., 1998). The multiplicity of these ν(OH) bands indicates that a large number of different types of OH groups (Thornton & Harrison, 1975; Harrison & Maunders, 1984; Emiroglu et al., 2001) exist at the surface of the SnO₂ nanoparticles. Indeed, the different vibrational frequencies of the OH groups originate

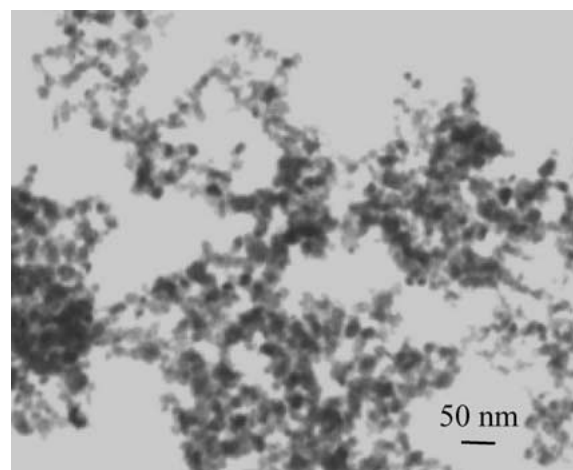


Figure 2. TEM analysis of the SnO₂ nanoparticles.

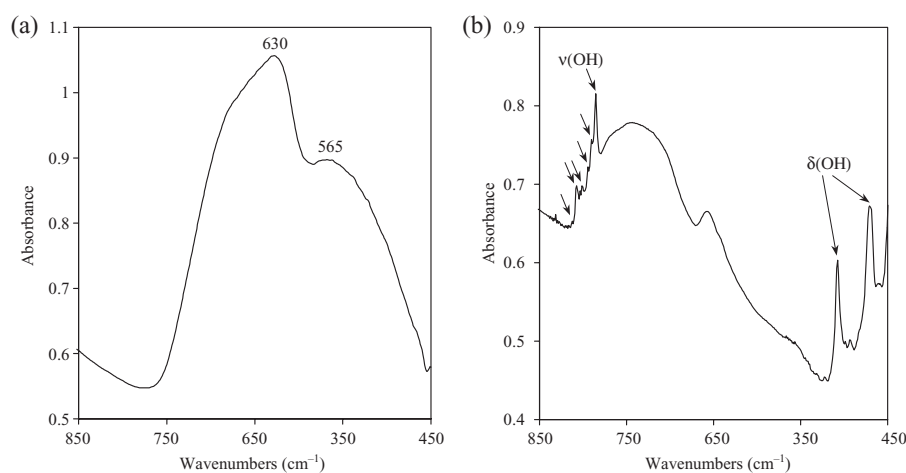


Figure 3. Infrared transmission spectra of the SnO_2 nanoparticles: (a) spectrum of the bulk; (b) spectrum of the surface chemical species (the different $\nu(\text{OH})$ bands in the $4000\text{--}3000\text{ cm}^{-1}$ region are indicated by arrows).

from the diversity of the coordination types of the surface tin atoms to which the OH groups are bonded. For example, it is known that Sn^{2+} and Sn^{4+} along with oxygen vacancies can be present on the tin oxide surface (Cox et al., 1988; Henrich & Cox, 1994), thus generating different electronic distributions in the attached OH groups. It should be noted that all these OH surface groups may have different acido-basicity, that is different reactivity. It is therefore easy to understand that a reproducibility study of these $\nu(\text{OH})$ bands is critical to ensure a perfect reproducibility of the surface chemical composition and of the surface chemistry of the nanoparticles.

Rapid screening of the sensing potentiality of the nanoparticles

As the deposition technique is a relatively time-consuming process, a methodology was established to rapidly screen the semiconducting nanoparticles in terms of gas sensing potentiality before embarking in the fabrication of the devices. This rapid screening is based on the analysis of the absorption of the free carriers in the whole infrared range (Harrick, 1962). Indeed, while surface infrared spectroscopy allows the characterization of the chemical nature of the surface species and the identification of the bonding sites, absorption due to surface electronic phenomena represents an intrinsic part of the infrared spectrum of semiconductors. The semiconducting property originates from the mobility of free carriers (electrons in n-type or holes in p-type semiconductors) and, according

to the Drude–Zener theory (Gibson, 1958; Harrick, 1967), these free carriers contribute to the absorption by the material over the whole infrared range. The absorption of the free carriers has been ignored in vibrational studies because it is very broad compared to the sharp vibrational bands (Chabal, 1988). But it has been experimentally demonstrated that the variations of the background infrared absorption of a semiconductor sample reflect the variations of the free carrier density, that is the variations of the electrical conductivity (Harrick, 1962). In previous works, we proved that the variations of the infrared energy transmitted by the semiconductor nanoparticles *versus* gas exposures could be directly related to the electrical response of the real sensor (Baraton, 2000; 2002; Baraton & Merhari, 2000; 2001b). Because FTIR spectroscopy is also a convenient tool to follow *in situ* the reactions at the nanoparticle surface (Baraton et al., 2000), it becomes clear that FTIR surface spectroscopy is an excellent method to fundamentally study the gas detection mechanisms taking place in semiconductor-based sensors. It must be stressed that, in this particular case, FTIR spectrometry combines the investigations of two related phenomena (surface reactions and electrical conductivity) involving different thicknesses of the material because the surface reactivity concerns only the first atomic layer whereas the thickness variation of the depletion layer may concern up to several tens of nanometers.

As an example, Figure 4 shows the infrared spectrum of the tin oxide nanoparticles recorded at 300°C under oxygen (spectrum a). When carbon monoxide

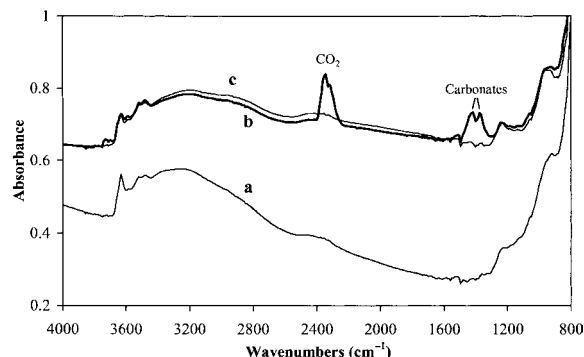
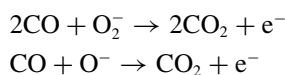
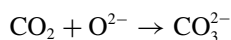


Figure 4. Infrared spectrum of the SnO₂ nanoparticles at 300°C: (a) under 50 mbar oxygen; (b, bold line) after addition of 10 mbar CO in presence of oxygen; (c) after evacuation.

is adsorbed on the surface in presence of oxygen, an increase of the background absorbance is observed, caused by an increase of the free carrier density corresponding to an electrical conductivity increase (spectrum b). This increase of the electron density is due to the oxidation of carbon monoxide into carbon dioxide by reaction with ionsorbed oxygen at the tin oxide surface (Clifford, 1981; Henrich & Cox, 1994). In this reaction, electrons, which are the free carriers in this n-type semiconductor, are released into the conduction band as follows:



The absorption band of gaseous carbon dioxide is indeed noted on the infrared spectrum at 2348 cm⁻¹ (spectrum b). Carbonate surface groups are subsequently formed by adsorption of the resulting CO₂ on basic surface sites without any change in the electrical conductivity:



The absorption bands of the carbonate species are observed in the 1450–1350 cm⁻¹ region (spectrum b). Both carbon dioxide and carbonate groups are eliminated by evacuation (spectrum c), thus showing the reversibility of the reactions. This reversibility, ensuring the stability of the sensor baseline, is a necessary condition for proper sensor operation.

In Figure 5, the variations of the infrared energy (E_{IR}) transmitted by the SnO₂ nanoparticles are reported versus gas exposures. An increase of the transmitted infrared energy (i.e. a decrease of the overall absorbance) corresponds to a decrease of the

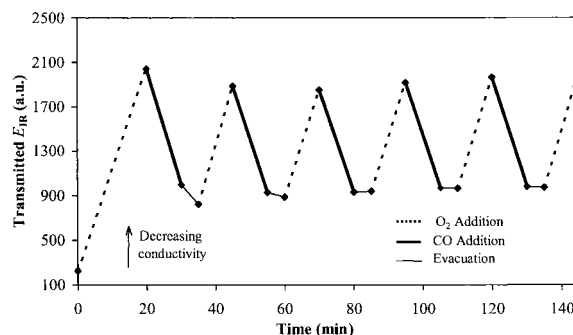


Figure 5. Variations of the infrared energy (E_{IR}) transmitted by the SnO₂ nanoparticles versus gas exposures at 300°C. An increase of E_{IR} is due to a decrease of the electrical conductivity.

electrical conductivity. Reproducible variations of E_{IR} are observed under carbon monoxide additions in presence of oxygen. As mentioned above, such a curve has been proved to directly correspond to the electrical response of the real sensor (SMOGLESS Final Report, 1999; Baraton & Merhari, 2001b; Baraton, 2002).

This type of infrared analysis of semiconducting nanoparticles appeared to be extremely useful to get a relatively quick evaluation of the sensing potentiality of the materials as soon as they are synthesized. It also allows a fundamental study of the surface reactions at the origin of the gas detection mechanism, thus making it possible to tailor the surface chemistry for maximizing the efficiency of these reactions responsible for the electrical conductivity variations. By optimization closed-loops, it was then possible to rapidly adjust the synthesis parameters for optimized sensing properties and to select the best batches of nanoparticles to be further processed.

First optimization stage of the screen-printing process

During the first optimization stage of the screen-printing process, a homogeneous dispersion of the nanoparticles in the solvent (essentially α -terpineol) was achieved by determining the appropriate concentration and by applying ultrasonication before screen-printing. Then, from SEM analysis and systematic electrical measurements, it was observed that the sintering temperature had a strong influence on the grain growth and also on the sensor sensitivity. It was found that up to 450°C the grain growth was not significant but rapidly increased above this temperature. The sintering temperature was set below this

critical value (around 400°C for SnO₂ films), but may vary depending on the metal oxide. When appropriate, a catalyst (such as Pd or Pt, depending on the gas to be detected) was added to the metal oxide to increase both sensitivity and selectivity at lower operating temperature.

With this deposition technique, a film with a thickness down to less than 1 μm could be obtained. Further fundamental investigation showed that the porosity of the sensitive layer had to be controlled through adjustment of the particle size distribution and of the firing temperature. It was indeed found that the porosity and the pore volume curves of the sensitive layer had a similar shape to that of the sensor sensitivity curve (Willett et al., 1998).

Table 2 compares the sensitivity that our sensor prototypes could achieve at the end of this first optimization stage (in 2000) with both the targeted sensitivities and the sensitivities of the electrochemical and semiconductor sensors commercially available at that time. It was clear that neither the commercial sensors nor our prototypes could meet our targets for outdoor AQM.

However, our prototypes exhibited a detection threshold to ozone, NO and NO₂ comparable to that of the electrochemical cells which, as previously mentioned, are very sensitive but much more expensive than semiconductor sensors. As for our CO sensor prototype, it appeared more sensitive than its Figaro counterpart.

Second optimization stage of the screen-printing process

To further optimize our devices, we had to come up with a new concept of fabrication better accommodating the nanoparticles. The goal was to obtain homogeneous stacked layers of nanoparticles. As explained above, it was thought that the suppression of agglomerates

should lead to improved adhesion, improved film quality, more homogeneous pore size and pore distribution and that a narrower particle size distribution should lead to a higher surface to bulk ratio and therefore to a higher sensitivity to gases. Additionally, a monolayer of nanoparticles deposited onto a substrate should facilitate the formation of necks between the particles, thus ensuring better sensor performance. However, as previously seen from the TEM pictures (Figure 2), the nanoparticles were agglomerated and ultrasonication could be insufficient to achieve a complete deagglomeration of the nanoparticles in the solvent.

Because industrial considerations precluded the manipulation of nanoparticles one by one, we developed a low-cost layer-by-layer deposition method via a wet route where the nanoparticles would preferably pile up in a regular 3D network thanks to their identical size.

The layer-by-layer deposition method consisted in dispersing the nanoparticles in an appropriate solvent to obtain a very diluted colloid. After sedimentation during a few hours, a drop of the supernatant was taken and deposited onto the alumina tile. The thin layer of nanoparticles was allowed to dry before a subsequent layer was deposited. The procedure was repeated up to 100 times then the sensor was heat-treated below 450°C. The final film was almost transparent under white light.

Figures 6 and 7, respectively, show the sensitivity to NO₂ and to ozone of our sensor prototypes based on 15 nm tin oxide particles and fabricated by the layer-by-layer deposition method. As a reminder, the sensitivity is expressed as the ratio of the resistance of the sensors under synthetic air and under synthetic air mixed with various concentrations of the gas to be detected. The optimized operating temperatures were determined to be 140°C for NO₂ and 120°C for ozone detection.

Table 2. Comparison between our targeted detection thresholds, the gas detection thresholds of commercial sensors and the gas detection thresholds of our sensor prototypes at the end of the first optimization stage (2000)

Polluting gases	Target for the detection threshold	Detection thresholds of commercial sensors (typical data available in 2000)		Our sensor prototypes (1st optimization round; 2000)
		Semiconductor	Electrochemical	
CO	3 ppm	100 ppm	5 ppm	30 ppm
NO ₂	50 ppb		600 ppb	500 ppb
NO	100 ppb		900 ppb	800 ppb
O ₃	20 ppb		200 ppb	200 ppb

The threshold detection limit was about 15 ppb for both gases. The response time was of the order of 1 min in both cases. Obviously, this response time is much too long, and particularly if the sensors have to be used in mobile microstations. However, further investigation showed that a shorter response time would be difficult to achieve because of the limitation imposed by

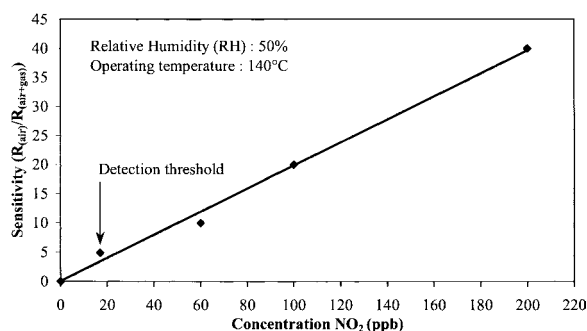


Figure 6. Sensitivity of our sensor prototype based on 15 nm-SnO₂ toward NO₂ after the second optimization stage (2002) (Adapted from ref. INTAIRNET Second-Year Report, 2002).

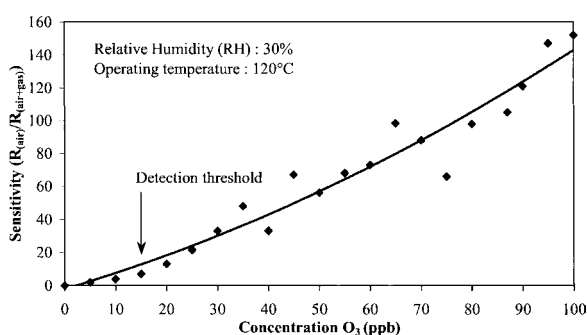


Figure 7. Sensitivity of our sensor prototype based on 15 nm-SnO₂ toward ozone after the second optimization stage (2002) (Adapted from ref. INTAIRNET Second-Year Report, 2002).

the reaction rate at the surface of the semiconductor under extremely low gas concentrations. This problem has nevertheless been overcome by an appropriate electronic design.

Table 3 gives the lowest gas concentrations that our sensor prototypes could reliably detect at the end of the second optimization stage (achieved in 2002). The detection thresholds are compared to the targets previously defined and to the typical detection thresholds of commercial sensors as available in 2002.

The obvious conclusion is that our sensors can compete with commercial devices. But more important, our sensors can fully meet the required targets for outdoor AQM whereas commercial electrochemical and semiconductor sensors still cannot.

Outlook

Our Consortia showed that nanoparticles-based semiconductor sensors exhibit higher sensitivities to air pollutants, lower detection thresholds, lower operating temperatures. The device optimization is not a straightforward procedure and requires controlled surface chemistry of nanoparticles, homogeneous dispersion of nanoparticles, deposition of homogeneous layers, a low level of dopant if any and mild firing conditions. All the results have been achieved thanks to the complementary expertises of the research teams closely collaborating for several years within these two European projects. Tight coordination of the research efforts and rigorous consolidation of the results provided by each team were also necessary steps toward successful achievements.

Although our sensors are chemically and electrically stable, the long-term stability over extended periods of time (several months) has still to be checked. The response time of our sensor prototypes is typically

Table 3. Comparison between our targeted detection thresholds, the gas detection thresholds of commercial sensors and the gas detection thresholds of our sensor prototypes after the second optimization stage (2002)

Polluting gases	Target for the detection threshold	Detection thresholds of commercial sensors (typical data available in 2002)		Our sensor prototypes (2nd optimization round; 2002)
		Semiconductor	Electrochemical	
CO	3 ppm	5 ppm	1 ppm	3 ppm
NO ₂	50 ppb		100 ppb	15 ppb
NO	100 ppb		500 ppb	50 ppb
O ₃	20 ppb		50 ppb	15 ppb

of the order of 1 min at the lowest gas concentrations. However, we have come up with an electronic design which will allow the measurement of gas concentrations every 10 or 20 s. Independently from but simultaneously with the optimization of the sensing layer, the cross-sensitivity to humidity which is a critical issue for semiconductor sensors was addressed. The resulting whole sensing unit which is small enough to be a portable device will be able to reliably operate under a relative humidity (RH) varying from 10% to 100% and an outdoor temperature varying from 5°C to 60°C (INTAIRNET Second Year Report, 2002). This sensing unit associated with GPS and GSM powered by a battery constitute our proposed portable AQM microstation to be implemented on mobile carriers.

As previously explained, our proposed dynamic network is relevant only if semiconductor sensors are capable of successfully and reliably detecting low gas concentrations, which represented the most important challenge in our concept of mobile AQM microstations. We have now proved that these low-cost gas sensors can meet the criteria in terms of detection thresholds for polluting gases in air. Our concept can now proceed with the complete development of the AQM microstations which could be implemented easily, rapidly and in a sufficient number in any city of any country at low cost.

Acknowledgements

The authors and more particularly the coordinator of the two projects (MIB) are indebted to their partners in the SMOGLESS and INTAIRNET Consortia and more specifically to Drs. W. Riehemann, H. Ferkel and J.F. Castagnet (IWW, Technische Universität Clausthal, Clausthal-Zellerfeld, Germany) for the synthesis of nanoparticles, to Drs. G.S.V. Coles, G. Williams and T. Starke (University of Wales at Swansea, UK) for the sensors fabrication and their electrical characterization, to Drs. V. Burganos and S. Zarkanitis (ICE-HT/FORTH, Patras, Greece) for their studies of the porosity influence and of the cross-sensitivity to humidity, to Drs. M. Taylor and L. Witrant (Oldham-France S.A., Arras, France), Drs. M. Willett and M. Jones (City Technology Ltd, Portsmouth, UK) for the sensors evaluation under industrial conditions. The financial support of the European Commission under the BRITE-EURAM III and IST programs is gratefully acknowledged.

References

- Baraton M.-I., 1999. In: Nalwa H.S. ed. Handbook of Nanostructured Materials and Nanotechnology; FT-IR Surface Spectrometry of Nanosized Particles. Academic Press, San Diego, pp. 89–153.
- Baraton M.-I., 2000. In: Chow G.-M., Ovid'ko I.A. and Tsakalakos T. eds. Nanostructured Films and Coatings; Surface Characterization of Nanostructured Coatings: Study of Nanocrystalline SnO₂ Gas Sensors, NATO-ARW Series, Kluwer Academic Publishers, Dordrecht, pp. 187–201.
- Baraton M.-I., 2002. In: Knauth P. and Schoonman J. eds. Nanocrystalline Metals and Oxides: Selected Properties and Applications; Surface Analysis of Semiconducting Nanoparticles by FTIR Spectroscopy: Application to the Evaluation of Gas Sensing Properties. Kluwer Academic Publishers, Boston, pp. 165–187.
- Baraton M.-I. & L. Merhari, 1998. Surface properties control of semiconducting metal oxides nanoparticles. *NanoStruct. Mater.* 10, 699–713.
- Baraton M.-I. & L. Merhari, 2000. In: Komarneni S., Parker J.C. and Hahn H. eds. Nanophase and Nanocomposite Materials III; Chemical Reactions on the Surface of SnO₂ Nanosized Powders at the Origin of the Gas Sensing Properties: FTIR Investigation, MRS Symposium Proceeding Series Vol. 581. MRS Publisher, Warrendale, pp. 559–564.
- Baraton M.-I. & L. Merhari, 2001a. Influence of the particle size on the surface reactivity and gas sensing properties of SnO₂ nanopowders. *Mater. Trans.* 42, 1616–1622.
- Baraton M.-I. & L. Merhari, 2001b. Determination of the gas sensing potentiality of nanosized powders by FTIR spectrometry. *Scripta Mater.* 44, 1643–1648.
- Baraton M.-I., L. Merhari, H. Ferkel & J.F. Castagnet, 2002. Comparison of the gas sensing properties of tin, indium and tungsten oxides nanopowders: Carbon monoxide detection and humidity effects. *Mater. Sci. Eng. C* 19, 315–321.
- Chabal Y.J., 1988. Surface infrared spectroscopy. *Surf. Sci. Rep.* 8, 211–357.
- Chancel F., J. Tribout & M.-I. Baraton, 1998. In: Gonsalves K.E., Baraton M.-I., Singh R., Hofmann H., Chen J.X. and Akkara J.A. eds. Surface Controlled Nanoscale Materials for High-Added-Value Applications; Effect of Surface Modification on the Electrical Properties of TiO₂ and SnO₂ Nanopowders, MRS Symposium Proceeding Series Vol. 501. MRS Publisher, Warrendale, pp. 89–94.
- Clifford P.K., 1981. Mechanisms of Gas Detection by Metal Oxide Surfaces. Ph.D. Thesis, Carnegie Mellon University, Pittsburg.
- Cox D.F., T.B. Fryberger & S. Semancik, 1988. Oxygen vacancies and defect electronic states on the SnO₂(110)-1 × 1 surface. *Phys. Rev. B* 38, 2072–2083.
- Emiroglu S., N. Bârsan, U. Weimar & V. Hoffmann, 2001. *In situ* diffuse reflectance infrared spectroscopy study of CO adsorption on SnO₂. *Thin Solid Films* 391, 176–185.
- Gibson A.F., 1958. Infrared and microwave modulation using free carriers in semiconductors. *J. Sci. Instrum.* 35, 273–278.
- Harrick N.J., 1962. Optical spectrum of the semiconductor surface states from frustrated total internal reflection. *Phys. Rev.* 125, 1165–1170.

- Harrick N.J., 1967. *Internal Reflection Spectroscopy*. Interscience, Wiley, New York.
- Harrison P.G. & B.M. Maunders, 1984. Tin oxide surfaces. Part 12. A comparison of the nature of tin(IV) oxide, tin(IV) oxide-silica and tin (IV) oxide-palladium oxide: Surface hydroxyl groups and ammonia adsorption. *J. Chem. Soc. Faraday Trans. I* 80, 1341–1356.
- Henrich V.E. & P.A. Cox, 1994. *The Surface Science of Metal Oxides*. Cambridge University Press, Cambridge.
- INTAIRNET Second Year Report (contract No. IST-1999-12615), 2002. Unpublished results.
- Morrison R.S., 1994. In: Sze S.M. ed. *Semiconductor Sensors; Chemical Sensors*, Chapter 8. John Wiley & Sons, New York, pp. 383–413.
- Ocaña M. & C.J. Serna, 1991. Variations of the infrared powder spectra of TiO₂ and SnO₂ (rutile) with polarization. *Spectrochim. Acta* 47A, 765–774.
- Ocaña M., C.J. Serna, J.V. Garcia-Ramos & E. Matijević, 1993. A vibrational study of uniform SnO₂ powders of various morphologies. *Solid State Ionics* 63–65, 170–177.
- Ogawa H., M. Nishikawa & A. Abe, 1982. Hall measurement studies and an electrical conduction model of tin oxide ultrafine particle films. *J. Appl. Phys.* 53, 4448–4455.
- Panchapakesan B., D.L. DeVoe, M.R. Widmaier, R. Cavicchi & S. Semancik, 2001. Nanoparticle engineering and control of tin oxide microstructures for chemical microsensor applications. *Nanotechnology* 12, 336–349.
- Riehemann W., 1998. In: Gonsalves K.E., Baraton M.-I., Singh R., Hofmann H., Chen J.X. and Akkara J.A. eds. *Surface Controlled Nanoscale Materials for High-Added-Value Applications; Synthesis of Nanoscaled Powders by Laser-Evaporation of Materials*, MRS Symposium Proceeding Series Vol. 501. MRS Publisher, Warrendale, pp. 3–14.
- Shimizu Y. & M. Egashira, 1999. Basic aspects and challenges of semiconductor gas sensors. *MRS Bull.* 24, 18–24.
- SMOGLISS Final Report (contract No.: BRPR-CT95-0002), 1999. Unpublished results.
- Somorjai G.A., 1994. *Introduction to Surface Chemistry and Catalysis*. John Wiley & Sons, New York.
- Thornton E.W. & P.G. Harrison, 1975. Tin oxide surfaces. Part 1. Surface hydroxyl groups and the chemisorption of carbon dioxide and carbon monoxide on tin(IV) oxide. *J. Chem. Soc. Faraday Trans. I* 71, 461–73.
- Tribout J., F. Chancel, M.-I. Baraton, H. Ferkel & W. Riehemann, 1998. In: Gonsalves K.E., Baraton M.-I., Singh R., Hofmann H., Chen J.X. and Akkara J.A. eds. *Surface Controlled Nanoscale Materials for High-Added-Value Applications; Oxygen Adsorption on Tin Oxide Nanosized Powders Characterized by FT-IR Spectrometry and Relation with the Sensor Properties*, MRS Symposium Proceeding Series Vol. 501. MRS Publisher, Warrendale, pp. 95–100.
- Willett M.J., V.N. Burganos, C.D. Tsakiroglou & A.C. Payatakes, 1998. Gas sensing and structural properties of variously pre-treated nanopowder tin (IV) oxide samples. *Sens. Actuators B* 53, 76–90.
- Williams G. & G.S.V. Coles, 1998. Gas sensing properties of nanocrystalline metal oxide powders produced by a laser evaporation technique. *J. Mater. Chem.* 8, 1657–1664.
- Williams G. & G.S.V. Coles, 1999. The gas-sensing potential of nanocrystalline tin dioxide produced by a laser ablation technique. *MRS Bull.* 24, 25–29.